

Reliability-based Topology Optimization for Offshore Wind Farm Collection System

Juan-Andrés Pérez-Rúa¹, Sara Lumbreras², Andrés Ramos², and Nicolaos A. Cutululis¹

¹DTU Wind Energy, Technical University of Denmark, Frederiksborgvej 399, 4000 Roskilde, Denmark

²Institute for Research in Technology, Comillas Pontifical University, Calle de Alberto Aguilera 23, 28015 Madrid, Spain

Correspondence: Juan-Andrés Pérez-Rúa (juru@dtu.dk)

Abstract. An optimization framework for global optimization of the cable layout topology for Offshore Wind Farm (OWF) is presented. The framework designs and compares closed-loop and radial layouts for the collection system of OWFs. For the former, a two-stage stochastic optimization program based on a **Mixed Integer Linear Programming (MILP)** model is developed, while for the latter, a hop-indexed full binary model is used. The purpose of the framework is to provide a common base for assessing both designs economically, using the same underlying contingency treatment. A discrete Markov model is implemented for calculating the cable failure probability, useful for estimating the time under contingency for multiple power generation scenarios. The objective function supports simultaneous optimization of: (i) initial investment (network topology and cable sizing), (ii) total electrical power losses costs, and (iii) operation costs due to energy curtailment from cables failures. Constraints are added accounting for common engineering aspects. The applicability of the full method is demonstrated by tackling three differently sized real-world OWFs. Results show that: (i) the profitability of either topology type depends strongly on the project size and wind turbine rating. Closed-loop may be a competitive solution for large-scale projects where large amounts of energy are potentially curtailed. (ii) The stochastic model presents low tractability to tackle large-scale instances, increasing the required computing time and memory resources. (iii) Strategies must be adopted in order to apply stochastic optimization for modern OWFs, intending analytically or numerically simplification of mathematical models.

Nomenclature

Acronyms

OWF(s) Offshore Wind Farm(s).

LCOE Levelised Cost Of Energy.

BoP Balance of Plant.

WT(s) Wind Turbines(s).

OSS(s) Offshore Substation(s).

MILP Mixed Integer Linear Programming.

MIQP Mixed Integer Quadratic Programming.

MINLP Mixed Integer Nonlinear Programming.

NP Non-Deterministic Polynomial.

PCI Progressive Contingency Algorithm.

MTBF Mean Time Between Failures.

MTTF Mean Time To Repair.

DC Direct Current.

Parameters (non-sets)

n_w Number of wind turbines.

d_{ij} Euclidean norm for edge $[ij]$.

v Number of wind turbines connectable to each wind turbine.

σ Maximum number of main feeders.

u_t Capacity of cable t in Amperes.

c_t Metric capital and installation cost of cable t .

R_t Metric electrical resistance of cable t .

X_t Metric electrical reactance of cable t .

ω_n Nominal wind power generation scenario.

k_o Base system state.

τ^ω Duration of wind power generation scenario ω in hours.

ζ^ω Magnitude of wind power generation scenario ω in p.u.

ψ^k Probability of system state k .

r_e Reliability level.

r_{ij}^k Control parameter for edge $[ij]$ availability.

I_i^ω Current generated at wind turbine i in scenario ω .

V_n Nominal line-to-line voltage of the system.

P_n Nominal power of the wind turbines.

U Capacity of the biggest cable available in number of wind turbines.

c_e Cost of energy in Euro Ah^{-1} .

f_t Capacity of cable t in number of wind turbines.

ϵ_d Optimality gap for deterministic phase.

ϵ_s Optimality gap for stochastic phase.

κ_{\max} Maximum number of iterations for PCI algorithm.

Parameters (sets)

N_w Set of wind turbines.

N Set of offshore substation and wind turbines.

G Weighted undirected graph.

E Set of available edges.

D Set of edges weight.

T Set of available cables.

U Set of cables capacity in Amperes.

C Set of cables capital and installation cost.

Υ System scenario tree.

Ω Set of wind power generation scenarios.

K Set of system states.

T' Set of available cables when considering losses.

U' Set of cables capacity when considering losses.

Variables

y_{ij} Binary variable to activate edge $[ij]$.

$x_{ij,t}$ Binary variable to select optimum cable type t

$I_{ij}^{\omega,k}$ Continuous variable for current through edge $[ij]$ during system scenario $\{\omega, k\}$.

$\theta_i^{\omega,k}$ Continuous variable for voltage phase at busbar i during system scenario $\{\omega, k\}$.

$\delta_j^{\omega,k}$ Continuous variable for curtailed current at busbar i during system scenario $\{\omega, k\}$.

Optimization output (sets)

X_d Set of active variables $x_{ij,t}$ for deterministic phase.

Y_d Set of active variables y_{ij} for deterministic phase.

K' Set of representative system states.

E' Set of selected edges of interest such as $E' \subset E$.

E''' Set of unused edges such as $E''' \subset E$.

$K_{E'}$ Set of system states linked to E' .

$K_{E'''}$ Set of system states linked to E''' .

E'_0 Set of cumulative solution variables E' .

X_{ws} Set of warm-starting point.

X Set of active variables $x_{ij,t}$ for stochastic phase.

Y Set of active variables y_{ij} for stochastic phase.

X_{rd} Set of active variables $x_{ij,t}$ for radial layout.

Y_{rd} Set of active variables y_{ij} for radial layout.

Subscripts

i Element in the set N .

j Element in the set N .

ij Edge $[ij]$.

t Cable type in the set T .

t' Cable type in the set T' .

Superscripts

ω Wind power generation scenario in Ω .

k System state in K .

Functions

$f(t')$ Function to calculate metric cost of cable type t' .

$g(t')$ Function to calculate metric resistance of cable type t' .

$h(t')$ Function to calculate cost of electrical losses of cable type t' .

$P^{\Omega, K}$ Stochastic optimization program.

$\Phi(E')$ Function to map from edges set to system states set.

$Q([X_{rd}, Y_{rd}])$ Recourse function.

1 Introduction

Medium voltage power cables are required for the cable layout of Offshore Wind Farms (OWFs). Cables represent at least 11% of the overall Levelised Cost Of Energy (LCOE), being one of the major cost element along with the wind turbine nacelles, foundations, and Offshore Substation (OSS).¹ Between 2018 and 2028, a total of 19,702 km of array cables are forecast to be installed, worth 5.36 billions of British pounds, turning power cables into the main component of the Balance of Plant (BoP).² However, power cables do not only have a sizeable impact over capital expenses, but also affect greatly the operation and performance of OWFs projects. These electrical components can be single points of failure, leading to strongly undesired contingencies.³ Shallow waters, buried depth, seabed terrain movements,⁴ electro-thermal stress,⁵ and harsh accessibility conditions for maintenance and reparation,⁶ are the differential factors in the context of OWFs. These particular characteristics give rise to higher failure rates of submarine cables compared to those reported by other offshore industries, such as oil and gas.^{7,8}

In contrast to transmission (with typical rated voltage equal or higher than 110 kV), collection systems (33 kV or 66 kV rated voltage) have been commonly designed in a deterministic fashion, i.e., considering no cable failure during the project lifetime. This has resulted in radial topology, i.e., without electrical redundancy - trees according to graph theory⁹- being the most common subject of study in literature in this context, and currently represents the most frequent choice by OWF developers. This is understandable as failure rates tend to increase with the voltage level and the length,⁴ both higher for the

OWF transmission system. However, this can drive to underestimation of the contingencies occurrence, and their effects due to potential cables failures in collection systems.

Moreover, further insights are gained by applying probabilistic techniques in reliability assessment. The possibility to consider several operation states is fundamental in robust designs. In this sense, cables for collection systems may also be designed to provide increased levels of reliability, generally resulting in closed-loop topologies. With the increase in OWFs installed capacities, the trend of moving towards subsidy-free operating regimes, and more and better data linked to cables failures rates, quantification of economic suitability of closed-loop or radial topology is becoming essential.

Radial topology for OWF collection system, following a deterministic strategy, falls into a standard class of computational problems, being classified in computational complexity as NP-Hard. Thus, scalability is the main challenge, as modern OWFs are in the order of hundreds of Wind Turbines (WTs). State-of-the-arts works^{10,11,12,13,14,15,16} have focused on developing new mathematical models solved through global optimization solvers. The main objective has been to tackle large problems, while incorporating into the models real-world constraints. Mixed Integer Quadratic Programming (MIQP), Mixed Integer Non-Linear Programming (MINLP), and Mixed Integer Linear Programming (MILP) are the most used types of models. Each of these mathematical formulations impose certain limitations on the physics modelling options. For instance, using flow-based MILP makes it more difficult to include the quadratic active power losses explicitly into the objective function. The commonly used power flow equations solved with e.g. the Newton-Raphson method cannot be considered in MILP or MIQP formulations, but with a MINLP. Likewise, linear-based formulations are generally computationally more efficient than quadratic or non-linear.

Closed-loop designs have been studied as well.^{17,18} However, in both, the closed-loop design is done in a deterministic manner. In the former,¹⁷ a MILP model is extended to support this constraint, and in the latter¹⁸ a two-layered optimization process is developed, where the sub-problem uses optimal dual variables of the continuous relaxation of the master problem to increase feasible points diversity. In both articles, the cable sizing is missing, together with very important constraints such as power flow modelling, and cables failures. In this regard, it becomes very hard to assess the economic benefits of designs with increased reliability.

Stochastic optimization for OWFs electrical cable optimization has been addressed previously.^{19,20,21} Nonetheless, the focus of these articles is the holistic design for small-scale farms, while excluding practical engineering constraints such as no-crossing of cables, topological aspects, among others. The first work in the field¹⁹ proposed a MIQP model using exhaustive uncertainty enumeration. This work is continued by Lumbreras and Ramos,^{20,21} where the contribution is the development of techniques to accelerate the convergence to obtain solution through decomposition techniques.

The main contributions of this work are: (i) development, testing, and application of an algorithmic framework to design collection system with a closed-loop structure, using global optimization, integrated with analytical methods for reliability assessment. (ii) development of a common framework to assess and compare economically topology optimization for OWFs, namely closed-loop vs radial layouts. For the first point, the algorithm is based upon a MILP model solved using a commercial solver, able to account for the three main optimization criteria in electrical network planning: investment, total electrical power losses, and reliability. For the second point, a recourse problem is solved using the radial design and the same underlying

stochastic considerations utilized for the closed-loop design. It is important to remark that strategies for tackling large instances are quantitatively analyzed and discussed as well.

2 Stochastic Optimization Model

2.1 Graph representation and model description

In this section the MILP optimization program for the closed-loop stochastic model is deployed.²² The model is formulated using connection decisions (binary) and flow (continuous) variables. The optimization program for the deterministic model used to design radial layouts is not presented as is available in a previous work of the first author.¹⁶ It is fundamentally a hop-indexed model using uniquely binary variables (for the case of single OSS). While the hop-indexed model is generally more efficiently solved, the flow model brings along more modelling flexibility and versatility.

The aim of the optimization is to design a closed-loop cable layout of the collection system for an OWF, i.e., to interconnect through power cables the n_w WTs to the available OSS, while providing a redundant power evacuation route for each turbine. Let $\mathbf{N}_w = \{2, \dots, 1 + n_w\}$. Besides, let the points set be $\mathbf{N} = \{1\} \cup \mathbf{N}_w$, where the element $i \in \mathbf{N}$, such as $i = 1$ is the OSS.

The Euclidean distance between the positions of the points i and j , is denoted by d_{ij} . These inputs are gathered in a weighted undirected graph $G(\mathbf{N}, \mathbf{E}, \mathbf{D})$, with \mathbf{N} being the vertex set, \mathbf{E} the set of available edges arranged as a pair-set, and \mathbf{D} the set of associated euclidean distances for each element $[ij] \in \mathbf{E}$, where $i \in \mathbf{N} \wedge j \in \mathbf{N}$.

In general, $G(\mathbf{N}, \mathbf{E}, \mathbf{D})$ is a complete undirected graph. It may be bounded by defining uniquely those edges connecting the $v < n_w$ closest WTs to each WT, and by the $\sigma < n_w$ edges directly reaching the OSS from the WTs (also known as the main feeders).

Likewise, let \mathbf{T} be a predefined list of available cable types, and \mathbf{U} be the set of cable capacities sorted in non-decreasing order as in \mathbf{T} , being measured in Amperes (A), such that u_t is the capacity of cable $t \in \mathbf{T}$. Furthermore, each cable type $t \in \mathbf{T}$ has a cost per unit of length, c_t (including capital and installation costs), in such a way that \mathbf{U} and \mathbf{T} are both comonotonic. The set of expenditures per meter is defined as \mathbf{C} .

After defining the graph representation of the problem, the designed model and its formulation is deployed. The model captures in the objective function the costs linked to Investment (cables' capital and installation costs), Electrical Losses (in a conservative and approximated fashion), and Reliability (cost of energy curtailment). The problem is formulated as a stochastic optimization program, modelled with two stages: first, the investment (construction), and second, the operation.

Uncertainty is represented by means of a system scenario tree (Υ), expressing simultaneously how the stochasticity is developing over time, the different states of the random parameters, and the definition of the non-anticipative decisions in the present. The set of wind power generation scenarios is Ω , while the system states are \mathbf{K} . The nominal generation scenario is ω_n , and the base system state (k_o) represents the case of no failures. The base case is therefore represented by the scenario $\{\omega_n, k_o\}$. A wind power generation scenario $\omega \in \Omega$ has associated a duration time τ^ω (in hours), and power magnitude ζ^ω (in p.u.), and each system state $k \in \mathbf{K}$, a system probability ψ^k , calculated using a discrete Markov model to define the probability for a

cable' complementary states: available, and unavailable.²³ In the same way, given the low failure rates of these components, a N-1 criterion must be considered in each system state.²⁴

The first stage variables, independent of the system scenarios, are the binary variables $x_{ij,t}$, and y_{ij} ; where $x_{ij,t}$ is equal to one if active edge $[ij]$ ($y_{ij} = 1$) uses cable type $t \in \mathbf{T}$. The second stage variables, which represent the system scenarios of Υ , are the continuous variables $I_{ij}^{\omega,k}$, $\theta_i^{\omega,k}$, and $\delta_i^{\omega,k}$.

The electrical current in edge $[ij]$ in wind power generation scenario $\omega \in \mathbf{\Omega}$, and system state $k \in \mathbf{K}$ is represented by $I_{ij}^{\omega,k}$. Likewise for each system scenario, the voltage phase and curtailed current at a WT busbar i are $\theta_i^{\omega,k}$ and $\delta_i^{\omega,k}$, respectively. Note that $\delta_i^{\omega,k}$ (in A) is bounded by the current generated at i in the same scenario, I_i^ω , where $I_i^\omega = \frac{P_n \cdot \zeta^\omega}{\sqrt{3} \cdot V_n}$, being P_n the nominal power of an individual WT, and V_n the line-to-line nominal voltage of the system.

2.2 Cost coefficients and objective function

Total electrical power losses are non-linear in function of the current. In that event, two distinctive mathematical expressions to support simultaneous optimization of: (i) investment and operation, and (ii) investment, operation and losses are deployed. Both objective functions keep the linear structure of the model and must be selected exclusively.

2.2.1 Neglecting total electrical power losses

The objective function in this case consists of a simultaneous valuation of the total initial investment plus reliability. The investment is intuitively computed as the sum of cables costs installed in each edge $[ij]$; on the other hand, reliability is quantified through the expectation of economic losses due to cables failures, as the result of undispached current (i.e. energy) from each WT. In this way, the objective function is formalized as:

$$\min \underbrace{\sum_{[ij] \in \mathbf{E}} \sum_{t \in \mathbf{T}} c_t \cdot d_{ij} \cdot x_{ij,t}}_{\text{Investment}} + \underbrace{c_e \cdot \sum_{i \in \mathbf{N}_w} \sum_{\omega \in \mathbf{\Omega}} \sum_{k \in \mathbf{K}} \tau^\omega \cdot \psi^k \cdot \delta_i^{\omega,k}}_{\text{Operation/Reliability: Expected curtailed current}} \quad (1)$$

Here c_e is the cost of energy in Euro Ah⁻¹ (equivalent to Euro MWh⁻¹). The sum of system states probabilities must be equal to one, $\sum_{k \in \mathbf{K}} \psi^k = 1$, given the mutually exclusive nature of the considered events (at most one cable is subject to failure, N-1 criterion). A system state k represents the failure of a single cable in an active edge $e \in \mathbf{E}$, therefore the system probability for the state ψ^k is considered equal to this failure probability. This implies that the availability probability of the other installed cables is considered to be equal to one in this scenario,¹⁹ representing a conservative approach as the value of the parameter ψ^k is slightly overestimated (the system probability is the multiplication of each installed cable state probability).

2.2.2 Considering total electrical power losses

Total electrical power losses are non-linear in function of the current, cable type, and total length.⁹ The designer must try to find a proper balance between modelling fidelity and optimization program complexity. A pre-processing strategy is proposed

in this manuscript in order to incorporate this factor into the objective function.

$$f_t = \left\lfloor \frac{\sqrt{3} \cdot V_n \cdot u_t}{P_n} \right\rfloor \quad \forall t \in \mathbf{T} \quad (2)$$

The set of cable capacities in terms of number of supportable WTs is defined in Eq. (2). Let the new cable type set be:

$$\mathbf{T}' = \left\{ \underbrace{1, 2, \dots, f_1}_{t_1}, \underbrace{f_1 + 1, \dots, f_2}_{t_2}, f_2 + 1, \dots, \underbrace{f_{|\mathbf{T}|-1} + 1, \dots, f_{|\mathbf{T}|}}_{t_{|\mathbf{T}|}} \right\} \quad (3)$$

This implies that \mathbf{T}' is the discretized form of the maximum capacity $U = \max U$. Note that this is translated into the creation of additional variables $x_{ij,t'} : t' \in \mathbf{T}'$. Likewise, if the *floor function* in Eq. (2) is replaced by a *decimal round down function*, and \mathbf{T}' is also discretized using the same decimal steps, then the number of variables will increase accordingly, to the benefit of gaining in accuracy for the cable capacities. In \mathbf{T}' is contained the non-dominated cable sub-types from \mathbf{T} ; this means that each cable sub-type $t' \in \mathbf{T}'$ is related to a cable type $t \in \mathbf{T}$, inheriting physical properties such as cost per meter (c_t), electrical resistance per meter (R_t), and electrical reactance per meter (X_t); as shown in Eq. (3). Acknowledging that the investment cost of a cable t exceeds the electrical power losses costs, then the selected cable sub-type to connect n WTs will always be the cheapest (smallest) cable with sufficient capacity, rather than a bigger one with lower electrical power losses as the electrical resistance decreases with size. As a consequence of the aforementioned, let a new cable capacities set be:

$$\mathbf{U}' = \{1, 2, \dots, f_1, f_1 + 1, \dots, f_2, f_2 + 1, \dots, f_{|\mathbf{T}|-1} + 1, \dots, f_{|\mathbf{T}|}\} \cdot \frac{P_n}{\sqrt{3} \cdot V_n} \quad (4)$$

Let the functions $f(t')$, and $g(t')$, calculate cost, and electrical resistance per meter for cable sub-type t' , respectively, which are inherited from a cable type t . Whereby, the objective function for simultaneous optimization of investment, electrical losses, and expected curtailed current is:

$$\min \sum_{[ij] \in \mathbf{E}} \sum_{t' \in \mathbf{T}'} \left(\overbrace{f(t') + 3 \cdot 1.5 \cdot g(t') \cdot \left(\frac{c_e}{\sqrt{3} \cdot V_n} \right) \cdot \sum_{\omega \in \mathbf{\Omega}} (u_{t'}^\omega \cdot \zeta^\omega)^2 \cdot \tau^\omega}_{=h(t'). \text{ Pre-processing for total electrical power losses}} \right) \cdot d_{ij} \cdot x_{ij,t'} + \quad (5)$$

Operation/Reliability: Expected curtailed current

$$c_e \cdot \sum_{i \in \mathbf{N}_w} \sum_{\omega \in \mathbf{\Omega}} \sum_{k \in \mathbf{K}} \tau^\omega \cdot \psi^k \cdot \delta_i^{\omega,k}$$

The factor $(3 \cdot 1.5)$ in Eq. (5) accounts the joule, screen and armouring losses for the three-phase system. The whole term for total electrical power losses ($h(t')$) is calculated for each $t' \in \mathbf{T}'$, before launching the MILP model into the external solver. Therefore, the objective function is a linear weighting of the desired targets: investment, electrical losses, and reliability.

As discussed previously, one of the tasks of the designer is to balance out modelling fidelity and optimization program complexity. The objective function in Eq. (5) is a linear function, thus the following simplifications are assumed: (i) integer

discretization in Eq. (3) which restricts the capacity of cables, and may cause overestimation of electrical losses. This can be diminished by decimal round down, and by increasing discretization steps in Eq. (4) at the expense of incrementing the number of variables correspondingly. (ii) Neglect of system states (cables failures) apart of the base state (no failures); however, this is the state with highest probability. (iii) Power flow estimation in a conservative fashion, i.e., overestimating the incoming power flow by neglecting the total power losses downstream. All those simplifications may impact the final layout, however their conservative nature means rather over-designing than impacting the robustness.

2.3 Constraints

The first stage constraints are first presented. These constraints are only defined by the first stage variables.

In case edge $[ij]$ is active in the solution, then one and only one cable type $t \in \mathbf{T}$ or $t' \in \mathbf{T}'$ must be chosen as in

$$\sum_{t \in \mathbf{T}} x_{ij,t} = y_{ij} \quad \forall [ij] \in \mathbf{E} \vee \sum_{t' \in \mathbf{T}'} x_{ij,t'} = y_{ij} \quad \forall [ij] \in \mathbf{E} \quad (6)$$

Note that in case total electrical power losses are considered, then the cable types set is \mathbf{T}' , otherwise \mathbf{T} ; same logic for \mathbf{U}/\mathbf{U}' , t/t' , and $u_t/u_{t'}$. This applies for the forthcoming mathematical expressions.

A closed-loop (sunflower petals) collection system topology is forced through

$$\sum_{\substack{j \in \mathbf{N} \\ j \neq i}} y_{ij} = 2 \quad \forall l \in \mathbf{N}_w : l = i \vee l = j \quad (7)$$

Limiting the number of feeders (upper limit of ϕ feeders) connected to the OSS is carried out by means of

$$\sum_{i \in \mathbf{N}_w} y_{ij} \leq \phi \quad j = 1 \quad (8)$$

The set χ stores pairs of edges $\{[ij], [uv]\}$, which are crossing each other. Excluding crossing edges in the solution is ensured by the simultaneous application of the next linear inequalities along with Eq. (6)

$$y_{ij} + y_{uv} \leq 1 \quad \forall \{[ij], [uv]\} \in \chi \quad (9)$$

The no-crossing cables restriction is a practical requirement in order to avoid hot-spots, and potential single-points of failure caused by overlapping cables.¹² Constraint (9) exhaustively lists all combinations of crossings edges. The constraints in (6) ensure that no active edges are crossing or overlapping between each other. These constraints thus link the variables y_{ij} and $x_{ij,t}$.

The second stage constraints are now deployed. These constraints are only defined by the second stage variables. They are defined by the flow conservation, which also avoids disconnected solutions, as per

$$\sum_{\substack{i \in \mathbf{N} \\ j \neq i}} I_{ji}^{\omega,k} - I_{ij}^{\omega,k} + \delta_j^{\omega,k} = I_j^{\omega} \quad \forall j \in \mathbf{N}_w \quad \forall \omega \in \mathbf{\Omega} \quad \forall k \in \mathbf{K} \quad (10)$$

The set of tender constraints, useful to link first and second stage constraints, are lastly presented.

DC power flow is forced with

$$I_{ij}^{\omega,k} - \frac{V_n \cdot (\theta_i^{\omega,k} - \theta_j^{\omega,k})}{\sqrt{3} \cdot X_t \cdot d_{ij}} - M \cdot (1 - x_{ij,t}) - M \cdot r_{ij}^k \leq 0 \quad \forall [ij] \in \mathbf{E} \quad t \in \mathbf{T} \quad \forall \omega \in \mathbf{\Omega} \quad \forall k \in \mathbf{K} \quad (11)$$

$$-I_{ij}^{\omega,k} + \frac{V_n \cdot (\theta_i^{\omega,k} - \theta_j^{\omega,k})}{\sqrt{3} \cdot X_t \cdot d_{ij}} - M \cdot (1 - x_{ij,t}) - M \cdot r_{ij}^k \leq 0 \quad \forall [ij] \in \mathbf{E} \quad t \in \mathbf{T} \quad \forall \omega \in \mathbf{\Omega} \quad \forall k \in \mathbf{K} \quad (12)$$

Where r_{ij}^k is a parameter equal to one if edge $[ij]$ is failed, or zero if otherwise, and M is a big enough number to guarantee feasibility for those inactive or failed components.

The cable capacities are not exceeded by including the next bilateral constraints.

$$\sum_{t \in \mathbf{T}} u_t \cdot x_{ij,t} \cdot (1 - r_{ij}^k) \geq I_{ij}^{\omega,k} \quad \forall [ij] \in \mathbf{E} \quad \forall \omega \in \mathbf{\Omega} \quad \forall k \in \mathbf{K} \quad (13)$$

$$\sum_{t \in \mathbf{T}} -u_t \cdot x_{ij,t} \cdot (1 - r_{ij}^k) \leq I_{ij}^{\omega,k} \quad \forall [ij] \in \mathbf{E} \quad \forall \omega \in \mathbf{\Omega} \quad \forall k \in \mathbf{K} \quad (14)$$

The current $I_{ij}^{\omega,k}$ may circulate either from i to j or viceversa. In case total electrical power losses are considered, for all scenarios, except the ones linked to k_o , the capacity u'_t is inherited from the cable type t . This is to avoid unnecessary energy curtailment. For the base system state, k_o , capacity u'_t must be taken from Eq. (4).

Finally, constraints in Eq. (15) to Eq. (19) define the nature of the formulation by the variables definition, a MILP program, denoted as $P^{\Omega, \mathbf{K}}$.

$$x_{ij,t} \in \{0, 1\} \quad \forall t \in \mathbf{T} \quad \forall [ij] \in \mathbf{E} \quad (15)$$

$$y_{ij} \in \{0, 1\} \quad \forall [ij] \in \mathbf{E} \quad (16)$$

$$-0.1 \leq \theta_i^{\omega,k} \leq 0.1 \quad \forall i \in \mathbf{N} \quad \forall \omega \in \mathbf{\Omega} \quad \forall k \in \mathbf{K} \quad (17)$$

$$-U \leq I_{ij}^{\omega,k} \leq U \quad \forall [ij] \in \mathbf{E} \quad \forall \omega \in \mathbf{\Omega} \quad \forall k \in \mathbf{K} \quad (18)$$

$$0 \leq \delta_i^{\omega,k} \leq I_i^{\omega,k} \quad \forall i \in \mathbf{N}_w \quad \forall \omega \in \mathbf{\Omega} \quad \forall k \in \mathbf{K} \quad (19)$$

3 Algorithmic Framework for the Stochastic Optimization Model: Determining the representative system states

Since the two-stage variables scale-up exponentially as a function of the scenario tree size, the representative systems states must be obtained.²² The basic version of the stochastic optimization program presented in Sect. 2 encompasses the full set E ; each element $[i,j]$ gives place to a system state k to form the system states set K .

Nevertheless, the actual selected edges in a solution (i.e. a feasible point satisfying the optimality criteria) is only a subset $E' \subset E$; let the complement set E'' contain the unused elements from E , and let define the subset $E''' \subset E''$. Hereafter, it is proved that any representative system states set containing at least the scenarios linked to E' ($K_{E'} = \Phi(E')$), using the transformation function Φ which maps from edges set to system states set), is necessary and sufficient to obtain the optimum in $P^{\Omega, K}$.

Let the necessary and sufficient set K' encompass:

$$K' = k_0 \cup K_{E'} \cup K_{E'''} \quad (20)$$

Where $K_{E'''}$ is the system states linked to the subset of unused edges E''' .

Axiom 1. *The second stage variables linked to unused elements are equal to the base system state*

$$\forall i \in N_w \quad \forall k \in K_{E'''} \quad \forall \omega \in \Omega, \quad \delta_i^{\omega, k} = \delta_i^{\omega, k_0}$$

An intuitive proposition is reflected in Axiom 1: *The curtailed currents in the system state of unused edges are the same than in the base system state.* This basically means that the failures of unused elements will not deteriorate the operation of the system.

From Eq. (1) it follows:

$$\begin{aligned} & \sum_{[i,j] \in E} \sum_{t \in T} c_t \cdot d_{ij} \cdot x_{ij,t} + c_e \cdot \sum_{i \in N_w} \sum_{\omega \in \Omega} \sum_{k \in K' \setminus \{k_0\}} \tau^\omega \cdot \psi^k \cdot \delta_i^{\omega, k} + \\ & c_e \cdot \sum_{i \in N_w} \sum_{\omega \in \Omega} \tau^\omega \cdot \left(1 - \sum_{k \in K' \setminus \{k_0\}} \psi^k \right) \cdot \delta_i^{\omega, k_0} \end{aligned} \quad (21)$$

Eq. (21) with Eq. (20) becomes:

$$\begin{aligned} & \sum_{[i,j] \in E} \sum_{t \in T} c_t \cdot d_{ij} \cdot x_{ij,t} + c_e \cdot \sum_{i \in N_w} \sum_{\omega \in \Omega} \sum_{k \in K_{E'}} \tau^\omega \cdot \psi^k \cdot \delta_i^{\omega, k} + \\ & c_e \cdot \sum_{i \in N_w} \sum_{\omega \in \Omega} \sum_{k \in K_{E'''}} \tau^\omega \cdot \psi^k \cdot \delta_i^{\omega, k} + c_e \cdot \sum_{i \in N_w} \sum_{\omega \in \Omega} \tau^\omega \cdot \left(1 - \sum_{k \in K_{E'}} \psi^k \right) \cdot \delta_i^{\omega, k_0} - \\ & c_p \cdot \sum_{i \in N_w} \sum_{\omega \in \Omega} \sum_{k \in K_{E'''}} \tau^\omega \psi^k \cdot \delta_i^{\omega, k_0} \end{aligned} \quad (22)$$

Eq. (22) with Axiom 1 becomes:

$$\begin{aligned}
& \sum_{[ij] \in \mathbf{E}} \sum_{t \in \mathbf{T}} c_t \cdot d_{ij} \cdot x_{ij,t} + c_e \cdot \sum_{i \in \mathbf{N}_w} \sum_{\omega \in \Omega} \sum_{k \in \mathbf{K}_{E'}} \tau^\omega \cdot \psi^k \cdot \delta_i^{\omega,k} + \\
& \cancel{c_e \cdot \sum_{i \in \mathbf{N}_w} \sum_{\omega \in \Omega} \sum_{k \in \mathbf{K}_{E''}} \tau^\omega \cdot \psi^k \cdot \delta_i^{\omega,k_o}} + c_e \cdot \sum_{i \in \mathbf{N}_w} \sum_{\omega \in \Omega} \tau^\omega \cdot \left(1 - \sum_{k \in \mathbf{K}_{E'}} \psi^k \right) \cdot \delta_i^{\omega,k_o} - \\
& \cancel{c_p \cdot \sum_{i \in \mathbf{N}_w} \sum_{\omega \in \Omega} \sum_{k \in \mathbf{K}_{E''}} \tau^\omega \cdot \psi^k \cdot \delta_i^{\omega,k_o}}
\end{aligned} \tag{23}$$

Equation (23) is analogous to Eq. (21) but with $\mathbf{K}' \setminus \{k_o\} = \mathbf{K}_{E'}$. This proves that *any set \mathbf{K}' containing at least the system states associated to all selected edges is sufficient and necessary to find the global optimum of the full problem $P^{\Omega, \mathbf{K}}$* . Conversely, any instantiation for which $\mathbf{K}' \subset \mathbf{K}_{E'}$ would lead to an underestimation of operational costs, ultimately causing falling into suboptimal. The proof also applies when including total electrical power losses (5).

This contingency structure opens the door for a Progressive Contingency Incorporation (PCI) strategy, aiming to find a proper set \mathbf{K}' . An improved PCI algorithm based on a previous work²⁰ is proposed in the Algorithm 1.

Algorithm 1 Progressive Contingency Incorporation (PCI) Algorithm

- 1: $[\mathbf{X}_d, \mathbf{Y}_d] \leftarrow \arg P^{\Omega, \mathbf{K}'} : \Omega = \omega_n, \mathbf{K}' = k_o$ with gap ϵ_d
 - 2: $\mathbf{E}' \leftarrow \mathbf{Y}_d = \{[ij]\} : y_{ij} = 1 \quad \forall [ij] \in \mathbf{E} : [ij] \text{ satisfies reliability level } r_c$
 - 3: $\mathbf{E}'_o \leftarrow \emptyset, \mathbf{X}_{ws} \leftarrow \mathbf{X}_d \cup \mathbf{Y}_d$
 - 4: **for** ($\kappa = 1 : 1 : \kappa_{max}$) **do**
 - 5: $\mathbf{A} \leftarrow \mathbf{E}' \cap \mathbf{E}'_o$
 - 6: **if** ($\mathbf{E}' == \mathbf{A}$) **then**
 - 7: *Break*
 - 8: **end if**
 - 9: $\mathbf{E}'_o \leftarrow \mathbf{E}' \cup \mathbf{E}'_o$
 - 10: $[\mathbf{X}, \mathbf{Y}] \leftarrow \arg P^{\Omega, \mathbf{K}'} : \Omega, \mathbf{K}' = \Phi(\mathbf{E}'_o) \cup k_o$ with initial point \mathbf{X}_{ws} and gap ϵ_s . $\Upsilon = \{\Omega, \mathbf{K}'\}$
 - 11: $\mathbf{E}' \leftarrow \mathbf{Y} = \{[ij]\} : y_{ij} = 1 \quad \forall [ij] \in \mathbf{E} : [ij] \text{ satisfies reliability level } r_c$
 - 12: $\mathbf{X}_{ws} \leftarrow \mathbf{X} \cup \mathbf{Y}$
 - 13: **end for**
-

In the first line a deterministic instance of the full problem is tackled. This means considering uniquely the scenario $\{\omega_n, k_o\}$. For this problem a valid assumption is to consider zero curtailed power. After this, the active edges of interest corresponding to the first stage optimization variables are stored as \mathbf{E}' , along with the obtained solution variables in \mathbf{X}_{ws} (where \mathbf{X}_d and \mathbf{Y}_d contains the solution sets corresponding to $x_{ij,t}$, and y_{ij} for the deterministic case, respectively). As no previous iteration has been conducted, cumulative solution variables are unavailable (\mathbf{E}'_o). Since the second stage variables express contingency scenarios of the components delimited by the first stage variables, the tree Υ uniquely considers the failure states associated to

those components. For the case presented in Algorithm 1, solely those feeders which satisfy the reliability level r_c , are subject to fail.

Parameter r_c defines the degree of connection towards the OSS, so for example, $r_c = 1$ brings along the main feeders (rooted at $i = 1$), and $r_c = 2$ includes the last ones together with the feeders connected to the main ones, and so on for $r_c > 2$, as shown in Fig. 1. By means of this parameter, the model can be further relaxed for large instances. A reliability level equal to one according to Fig. 1 would still represent at a large extent the consequences of all cables failures, as those main feeders are the one carrying the vast amount of energy compared to downstream connections. Thus, an important computational burden is avoided, while having a good representation of the system. This is backed up by the fact that cables under higher levels of electro-thermal stress present shorter lifetime.⁵

The Progressive Contingency Incorporation routine for stochastic analysis is started at line 4. The opening step is to intersect the current active edges set \mathbf{E}' , and the cumulative set \mathbf{E}'_0 . If the intersection set is equal to the current active edges \mathbf{E}' , then the process is terminated, otherwise more iterations are attempted. For the former case, the algorithm is stopped, with solution $[\mathbf{X}, \mathbf{Y}]$; for the latter case, the iterative process is continued to the subsequent iteration κ . Trivially, for $\kappa = 1$, $\mathbf{A} = \emptyset$. Therefore, in line 9 the union set is obtained to update \mathbf{E}'_0 . A new instance of the main problem is solved in line 10, using the initial point \mathbf{X}_{ws} (warm-start point), while considering the full wind power generation scenarios indicated by the user Ω , and the system states related to edges cumulatively installed in all iterations, ($\mathbf{K}' = \Phi(\mathbf{E}'_0)$).

When the Algorithm 1 converges, the scenario criterion is met: obtention of the proper set \mathbf{K}' ; meaning that all representative systems states have been already considered.

4 Optimization Framework

The full optimization framework is presented in Fig. 2. The main inputs for the framework can be divided as:

- Project-specific data, such as WTs and OSS location, rated power, wind power generation scenarios, Mean Time Between Failures (MTBF) for cables (in years kilometres per failure), and Mean Time To Repair (MTTR) for failed cables (in hours).
- Simulation settings, like cables' technical and economic parameters, macroeconomic information, including lifetime and price of energy, and required gap for the deterministic case (ϵ_d) and the stochastic phase (ϵ_s).
- Modelling choices, as reliability level (r_c), total electrical power losses incorporation (1 or 0), and DC power flow model (1 or 0).

A Markov Chain methodology is applied to calculate the probability for the unavailable state of a cable:²³

$$\psi^k = \frac{MTTR}{MTTR + MTBF \cdot \frac{8760}{d_{ij}}} \quad (24)$$

Where d_{ij} (in kilometres) is the edge length where the component is installed, and k the associated system state.

Continuing with the flowchart of Fig. 2, two different models are formulated to tackle independently the stochastic closed-loop and the deterministic radial designs. As discussed previously, the closed-loop optimization program is based on a flow MILP model, in contrast to the hop-indexed optimization program dedicated for the non-looped layout, chosen such as to enable comparison of topologies for large-scale problems utilizing the state-of-the-art approaches.

The closed-loop stochastic model is formulated in function of the required inputs, especially *Losses* and *DC*. The objective function and constraints are properly adapted to whether losses must be incorporated or not (See Sect. 2.2).

Similarly, two options for power flow are supported, transportation model ($DC == False$) and a DC power flow ($DC == True$). A transportation model is fundamentally the simplest of the ways to calculate the distribution of power in an electrical network. It abides the Kirchhoff's first law by keeping the current balance at each node. Contrarily, a DC power flow model includes in addition the Kirchhoff's second law, approximating the voltage magnitude to 1 p.u., and ignoring the reactive power flow.²⁵ The mathematical optimization program is notably relaxed by disregarding the DC power flow, which stress the model by creating additional variables. Finally, after the optimization program is formulated, this is sent to the Algorithm 1, obtaining the layout with linked investment and expected operation costs.

On the right branch of the flowchart, the radial model is formulated and solved accordingly to the previously proposed model.¹⁶ The obtained solution sets ($\mathbf{X}_{rd}, \mathbf{Y}_{rd}$, conserving the adopted nomenclature as in Sect. 3), are used to fix values of the flow model binary variables; simultaneously, Eq. (7) are modified as inequalities to allow a maximum number of connections to each WT. With this, a tree topology is converted into a feasible point of the model. Lastly, the flow model is reassembled after all these changes, and sent to the Algorithm 1. In other words, a recourse problem is tackled $Q([\mathbf{X}_{rd}, \mathbf{Y}_{rd}])$, defined as minimization of the expected costs (operation costs) given the scenario tree (Υ) obtained from the wind power generation scenarios Ω , and the system states linked to \mathbf{Y}_{rd} . This recourse problem is inexpensive computationally given that the binary values are provided in advance. The recourse problem related to the radial layout is always solved to optimality.

In the last step of the flowchart, the two solutions (closed-loop and radial) are compared in terms of total expenses, investment and expected operation costs. This flow of tasks guarantee a fair comparison between them, since firstly, the same stochastic reference frame is maintained after the reformulation blocks depicted in Fig. 2, and, secondly, the PCI algorithm is utilized equally.

5 Results

The computational experiments presented in this section have been carried out on an Intel Core i7-6600U CPU running at 2.50 GHz and with 16 GB of RAM. The chosen solver is IBM ILOG CPLEX Optimization Studio V12.7.1.²⁶ The experiments consist on three real-world cases aiming to test the proposed method for different problem sizes (small, large and very large), and WTs topological distribution (grid-based and coordinate-based). For all the following studies a MTTR of 30 days (720 h) is considered.²⁷ The price of energy is assumed to be fixed along the project lifetime with a value of 50 Euro MWh^{-1} (2.86 Euro Ah^{-1}), which is the average price in the last years.²⁸

The wind power generation scenarios are also equally fixed as per Table 1. Scenario 1 accounts for the nominal power (ω_n). The time duration of all the scenarios correspond to a project lifetime of 30 years. The magnitude and duration values lead to a capacity factor of 0.49, which is a reasonable value for modern offshore wind farms.

In general, the simulation results are dependant on several parameters, like the utilization of a discrete Markov model to calculate the failure probabilities given the failure statistical parameters MTBF and MTTR, and the considered price of energy, financial valuation method, project lifetime, cables set, cost functions, among others.

Other electrical information related to the power cables, such as electrical resistance per meter (R_t) and electrical reactance per meter (X_t), is available in a publicly available catalogue.²⁹

5.1 Small OWF: Ormonde

As a first case study the Ormonde OWF³⁰ is analyzed. This OWF presents a closed-loop layout in the collection system. Specific inputs for this case study are shown in Table 2.

To better understand the influence of different modelling choices for the model included Algorithm 1, several simulations and parametric sensitivities are carried out. They target power flow model, reliability level, and total electrical power losses.

Trough these case studies, the complexity of different modules of the model is understood, along with the gains obtained by them.

5.1.1 Power flow model

For this study, only the left branch of Fig. 2 is executed without considering losses. This means that results focus on closed-loop topology in this section. The objective is to compare a full version of the model (with $DC == True$), and a relaxed version ($DC == False$) employing a simple transportation power flow model. Besides this, the MTBF is varied from 10 to 178 years kilometres per failure, with the latter value being typical for OWFs medium voltage cables under operation today,⁴ aiming at quantifying the parametric impact of MTBF value. To reduce computational burden when evaluating low values of MTBF, a reliability level of $r_c = 1$ is considered. See Fig. 1.

Results are presented in Table 3. For each MTBF value, the difference of total costs between the DC power flow model and the transportation model is presented. Percentage values are calculated with respect to the power flow relaxation model. Furthermore, total expenses are split into investment and operations costs to analyze their behaviour in function of the MTBF value.

Naturally, the total expenses for the relaxed solutions is lower than the full model (DC power flow), but what it is important to see is the rather limited impact of this relaxation in terms of the objective function value. In the worst case, the DC power flow model provides a solution only 0.62% more expensive than the transportation model. The latter result corresponds for the typical value of MTBF reported for OWFs (MTBF of 178). The cost difference among the power flow models can be explained by inspecting the investment and operation costs. The transportation model results in cheaper designs, but this precisely causes higher operation costs.

When considering a full reliability level, for a MTBF of 178, the solution obtained with a DC power flow model is only 0.25% more expensive than the one from a transportation model. While the difference on investment costs is more or less the same as in Table 3 (0.77%), it is observed an increase in the operation costs difference (-7.37%), which balances out the capital investment disparity among both models. The increment of undischarged energy allows for reducing the total expenses difference; this is also expected to happen for lower MTBF values.

The possibility to neglect DC power flow allows for reducing the complexity of the model while still generating dual solutions (by neglecting the DC flow) close to a primal (feasible point for the full model). In closed-loop and meshed topologies the current follows the path with shortest electrical length, i.e., smallest equivalent electrical reactance. Thus, DC power flow requires extra variables modelling voltage phases as in Eq. (11) and Eq. (12). The strong similarity between radial and closed-loop topologies is due to, in the latter, only a single cable per circuit (interconnected chain of WTs) alters the radiality of the former.

The main benefit behind this relaxation is towards the application of the model for large-scale problem instances, or even for small ones with low optimality gap values ($\epsilon_d, \epsilon_s \leq 0.2\%$). In this article, the comparison between closed-loop and radial designs lies in the relative economic difference, while not in the concrete solutions (construction designs). The dual solutions can be fixed a posteriori by changing a subset of the installed cables. The latter is out of the scope of this article.

5.1.2 Reliability level

The full Algorithm 1 is now implemented. Based on the results of Sect. 5.1.1, the DC power flow model is discarded. In the same manner, total electrical power losses are deactivated and attention is concentrated to a simultaneous minimization of investment plus operation costs. Results for the lowest reliability level ($r_c = 1$), and for full reliability, are displayed in Fig. 3 and in Fig. 4, respectively.

A reliability level value equal to $r_c = 1$ is basically a relaxation of the full model. The latest being understood as an instantiation of Algorithm 1 with a large enough value of r_c , such as all installed cables of the OWF are included in the system states set, i.e., full reliability. See Fig. 1 for a graphical description of this concept.

For the reliability relaxation, in Fig. 3(a) the total cost comparison between the closed-loop and radial designs with increasing MTBF is illustrated. Meanwhile, the Fig. 3(b) displays the investment and operation costs difference. From Fig. 3(a), it can be observed that there is break-even point, for a MTBF of around 35, where the total cost of closed-loop and radial designs match.

To the left of the break-even point, the closed-loop layout always results as the overall cheapest solution, because despite a higher investment cost- See Fig. 3(b) (radial design is invariable to MTBF variations)-, it provides a redundant path for each WT, therefore the operation cost savings surpasses that increase (the installed cables for the main feeders are usually bigger as well). Additionally, in Fig. 3(b) one can see that the non-increasing trend of the investment costs is developed in a discrete manner, as for some consecutive values of MTBF the closed-loop design investment is maintained. The associated percentage difference of operation costs for not modified designs is also kept, as the failures frequency is equally diminished.

On the other hand, for MTBF larger than 35, the radial layout is the best alternative. After a large enough MTBF (in this case at around 50 years kilometres per failure), the failures probabilities drop considerably, meaning that the operation costs become

trivial, and hence the focus is merely on the investment costs reduction, which by its part has reached the minimum in the closed-loop alternative. The break-even point may be marginally affected by neglecting the DC power flow in the conservative side, as this value would move to the left. At MTBF of 178, the radial design is 6.62% cheaper than the closed-loop design as shown in Fig. 3(a).

A new set of experiments is conducted for full reliability of the Ormonde OWF. The main difference compared to $r_c = 1$ is reflected in Fig. 4(a), where the break-even point is moved towards the right of the plot to a value roughly equal to 130 years kilometres per failure. By allowing the whole set of installed cables to fail, the impact over the project economic performance is considerably augmented. In this case, for the worst reported value of MTBF (178 years kilometres per failure), the radial design is only 1.98% cheaper than the closed-loop layout, due to the increase of operation costs with almost the same required investment expense when compared to $r_c = 1$.

The impact of the reliability level on the computing time is presented in Fig. 5. The difference is of an order of magnitude, moving from seconds for $r_c = 1$ to (tens of) minutes for full reliability. The exponential complexity of the stochastic closed-loop model in function of the parameter MTBF is also noticeable. For MTBF inferior to 40, the computational resources become insufficient to tackle the problem for full reliability, as computing time and memory requirements escalate rapidly.

For large values of MTBF the Algorithm 1 takes advantage of the deterministic solution to feed up the stochastic model with a good starting point. This, together with low failure probability (as MTBF increases), helps conspicuously to accelerate the convergence of the model for optimum gaps. The PCI algorithm takes away a very important share of computational burden by simplifying the full problem. The savings on computing time are more evident for greater values of r_c as the number of candidate edges become larger.

5.1.3 Total electrical power losses

The left branch of Fig. 2 is implemented, in this case, activating the total electrical power losses ($Losses == True$) integrated into the objective function Eq. (5). A MTBF of 178 years kilometres per failure is considered, the transportation power flow mode is enabled ($DC == False$), and full reliability level is selected.

Results are displayed in Fig. 6. Particularly, Fig. 6(a) is associated to objective function Eq. (1), and Fig. 6(b) to Eq. (5). There are no significant differences between the two layouts.

A visual inspection of the layouts shows that the only difference is the swap of cables connected from WT 1 to WT 11 with those from WT 1 to WT 2 in Fig. 6(b) compared to Fig. 6(a). This alteration in the design can be explained given the conservative approach for losses calculation, and simultaneously, the degree of flexibility linked to a transportation model. In Fig. 6(b), which graph the base case, the current through WTs 9-16 and 30-31 is set to zero in the solution. This means that the calculated losses are an approximation in the conservative side, compared to a layout with splittable current through a DC power flow.

The main takeaway is that the total expenses of the layout in Fig. 6(a) (including total electrical power losses) is nearly the same as that from Fig. 6(b). The required computing time, however, is 16 times higher when including losses compared to a sole optimization of investment and operation costs. The proposed formulation is still more efficient than a MIQP. The

demonstration is out of the scope of this work, but computational experiments from the literature validate the efficiency of MILP compared to MIQP.¹⁹

5.2 Large OWF: Horns Rev 1

The second case study is Horns Rev 1 OWF.³¹ Inputs are shown in Table 4. The number of WTs for this case is equal to 80. Horns Rev 1 OWF presents a regular or grid-based layout, since WTs units are uniformly arranged in rows and columns without empty areas inside of the farm; as shown in the previous work,¹⁶ this type of layouts show a favorable condition in terms of computational complexity when designing the collection system, hence low values $\nu = 6$ and $\sigma = 10$ are most likely good enough to cover the global minimum. Larger values of these parameters may compromise the convergence of general purpose solvers. No losses and a transportation power flow mode are used.

Results for the lowest reliability level, i.e. $r_c = 1$, are shown in Table 5. The optimality gap for both deterministic and stochastic phases of Algorithm 1 are equal $\epsilon_d = \epsilon_s = 0.2\%$. Further experiments were done, intending to evaluate lower values of MTBF at these gaps, but computing time increased steeply (note that for MTBF of 90, required time is almost 360 min).

Going back to Fig. 3, the results of Table 5 indicate that the break-even point has been already crossed for MTBF of 90. This is because of the nearly equal percentage of difference in investment for MTBF of 90 in comparison to MTBF of 178. At this point, the radial layout is 0.80% cheaper than the closed-loop design. One can see that for MTBF of 178, the savings difference for Horns Rev 1 (-2.01%) has decreased substantially when compared to Ormonde, Fig. 3(a) (-6.62%), and being closer to Ormonde with full reliability, Fig. 4(a) (-1.98%). Performance cutback of the radial layout is due to the boost of curtailed energy as there are more WTs connected to a single feeder.

For full reliability analysis, the value of ϵ_d is fixed to 0.2% while ϵ_s is loose up to 4%. This is necessary as symmetric tight gaps lead to failed convergence due to lack of memory. Providing the optimal solution of the deterministic phase of Algorithm 1 helps to shorten to stochastic phase, taking into account that the base case is the scenario with the largest probability. Results are shown in Table 6 where it can be seen that the closed-loop design is a more cost-effective option than the radial layout, even with a rather high optimality gap of up to 4%.

Two important aspects must be highlighted: (i) the transportation model allows for optimizing large OWFs at the expense of an slight underestimation of design costs, but even given this uncertainty, both topologies would be still very close in terms of financial performance. Slightly lower values of MTBF would mean the closed-loop gains more and more value. (ii) A gap of 4% means that the closed-loop layout could be possibly cheaper, increasing then its margin compared to the radial counterpart.

5.3 Very large OWF: West of Duddon Sands

Last real-world case study is West of Duddon Sands OWF.³² This OWF has an irregular distribution of its 108 WTs (3.6 MW individual power) due to abnormal soil conditions. Given this particular features, larger values of ν and σ are set, as indicated in Table 7, in order to cover the global minimum according to the hop-indexed model for radial layout design (right branch of Fig. 2). The presented optimality gaps (ϵ_d and ϵ_s) represent the technical border considering the lowest reliability level, to obtain solutions within the computational limits. No losses and a transportation power flow mode are used.

The numerical results are given in Table 8. Similarly to Horns Rev 1 (Table 5 and Table 6), with MTBF of 178, the results indicate that a closed-loop design for West Duddon Sands would most likely pay off under full reliability, since for the lowest redundancy level the radial layout is only 0.67% cheaper. This is understandable based on the greater number of WTs and individual power, leading to more curtailed energy for the same failure. This comparison is upon the condition that the relative difference between the solutions is maintained, if a zero optimality gap is achieved simultaneously.

The resulted closed-loop and radial layouts are given in Fig. 7. As aforementioned, this wind farm presents empty areas in between the locations of the generation units, which seems to impact considerably the mathematical complexity of finding a solution for the collection system. Previous studies have shown that the proposed hop-indexed formulation seems to be more compact and therefore more efficiently solved by commercial solvers than a flow formulation.¹⁶ This fact is also reflected in this case study, where for the same gap (5%), the flow-based model requires almost double time than the full binary (0.45 h). For Ormonde and Horns Rev 1 the radial layouts were obtained almost instantaneously.

In addition, the hop-indexed model does not escalate nor with the size of cable set, neither with inclusion of total electrical power losses. However, the flow formulation provides important flexibility to the model such as energy curtailment (used in this case) or other aspects like, e.g. different WTs types (in terms of power rating).

6 Conclusions

The proposed method provides a global optimization model to solve the OWFs collection system, supporting a simultaneous minimization of investment, expected operational, and total electrical power costs, including contingencies due to cables failures. In spite of the currently rather low failure rates of collector cables failures, early stage in offshore projects maturity and the consequent scarcity of available data may mean that future very large OWF projects may face larger level of contingencies.

The main contribution of this manuscript is the development of an optimization framework to compare, in economic terms, closed-loop and radial layouts for modern OWFs. Several strategies are incorporated in the algorithmic scheme, in order to be able to study very large real-world problems, such as the use of a transportation power flow model instead of DC power flow or different reliability levels.

The proposed methodology has been applied to three different OWFs, from small to very large-scale. Results indicate that layouts with single redundancy may bring economic benefits when compared to non-redundant ones, in function of the instance size. For a small OWF the radial topology results as the best option, in contrast to large projects, where the closed-loop is seemingly a better techno-economic solution, when using failures rates available in literature.

Stochastic optimization with scenario numeration brings along a comprehensive consideration of the three main criteria for designing electrical networks; investment, electrical losses, and reliability. However, it also implies a lack a tractability which hardens the applicability for a larger set of problem types. Overall, the impact of medium voltage collector system cables failures is quantified in this article, showing the importance of developing methods which enable reliability analysis in the context of computational optimization. A Progressive Contingency Algorithm has been proposed in this direction.

References

- ¹ ORE Catapult. Wind farm costs, 2020.
- ² RenewableUK. RenewableUK - Project Intelligence, 2018.
- ³ ReNEWS. Rampion suffers cable fault, 2017.
- ⁴ John Warnock, David McMillan, James Pilgrim, and Sally Shenton. Failure Rates of Offshore Wind Transmission Systems. *Energies*, 12(14):1–12, 2019.
- ⁵ Juan-Andrés Pérez-Rúa, Kaushik Das, and Nicolaos A. Cutululis. Optimum sizing of offshore wind farm export cables. *International Journal of Electrical Power & Energy Systems*, 113(December 2019):982–990, 2019.
- ⁶ François Besnard, Katharina Fischer, and Lina Bertling Tjernberg. A model for the optimization of the maintenance support organization for offshore wind farms. *IEEE Transactions on Sustainable Energy*, 4(2):443–450, 2013.
- ⁷ CIGRE: Working Group B1.10. Update of service experience of HV underground and submarine cables. Technical report, 2009.
- ⁸ CIGRE: Working Group B1.21. Third-Party Damage to Underground and Submarine Cables. Technical report, 2009.
- ⁹ Juan-Andrés Pérez-Rúa and Nicolaos A. Cutululis. Electrical Cable Optimization in Offshore Wind Farms - A review. *IEEE Access*, 7(1):85796–85811, 2019.
- ¹⁰ Yingying Chen, Zhao Yang Dong, Ke Meng, Fengji Luo, Zhao Xu, and Kit Po Wong. Collector System Layout Optimization Framework for Large-Scale Offshore Wind Farms. *IEEE Transactions on Sustainable Energy*, 7(4):1398–1407, 2016.
- ¹¹ Alain Hertz, Odile Marcotte, Asma Mdimagh, Michel Carreau, and François Welt. Design of a wind farm collection network when several cable types are available. *Journal of the Operational Research Society*, 68(1):62–73, 2017.
- ¹² Joanna Bauer and Jens Lysgaard. The offshore wind farm array cable layout problem: A planar open vehicle routing problem. *Journal of the Operational Research Society*, 66(3):360–368, 2015.
- ¹³ Martina Fischetti and David Pisinger. Optimizing wind farm cable routing considering power losses. *European Journal of Operational Research*, 270(3):917–930, 2018.
- ¹⁴ A. C. Pillai, J. Chick, L. Johanning, M. Khorasanchi, and V. De Laleu. Offshore wind farm electrical cable layout optimization. *Engineering Optimization*, 47(12):1689–1708, 2015.
- ¹⁵ Arne Klein and Dag Haugland. Obstacle-aware optimization of offshore wind farm cable layouts. *Annals of Operations Research*, 272(1-2):373–388, 2017.
- ¹⁶ Juan-Andrés Pérez-Rúa, Mathias Stolpe, Kaushik Das, and Nicolaos A. Cutululis. Global Optimization of Offshore Wind Farm Collection Systems. *IEEE Transactions on Power Systems*, 35(3):2256–2267, 2020.
- ¹⁷ Martina Fischetti and David Pisinger. Mixed Integer Linear Programming for new trends in wind farm cable routing. *Electronic Notes in Discrete Mathematics*, 64:115–124, 2018.
- ¹⁸ Arne Klein and Dag Haugland. Optimization of reliable cyclic cable layouts in offshore wind farms. *Engineering Optimization*, 52(3):1–20, 2020.
- ¹⁹ M Banzo and A Ramos. Stochastic Optimization Model for Electric Power System Planning of Offshore Wind Farms. *IEEE Transactions on Power Systems*, 26(3):1338–1348, 2011.
- ²⁰ Sara Lumbreras, Andres Ramos, and Santiago Cerisola. A Progressive Contingency Incorporation Approach for Stochastic Optimization Problems. *IEEE Transactions on Power Systems*, 28(2):1452–1460, 2013.

- ²¹ Sara Lumbreras and Andres Ramos. Optimal design of the electrical layout of an offshore wind farm applying decomposition strategies. *IEEE Transactions on Power Systems*, 28(2):1434–1441, 2013.
- ²² Juan-Andrés Pérez-Rúa, Sara Lumbreras, Andrés Ramos, and Nicolaos A. Cutululis. Closed-loop two-stage stochastic optimization of offshore wind farm collection system. *Journal of Physics: Conference Series*, 1618:042031, September 2020.
- ²³ Eduardo Calixto. *Gas and Oil Reliability Engineering*. Gulf Professional Publishing, second edition, 2016.
- ²⁴ Roy Billinton and Ronald N. Allan. *Reliability Evaluation of Engineering Systems: Concepts and Techniques*. 1992.
- ²⁵ John J Grainger and William D Jr Stevenson. *Power System Analysis*. McGraw-Hill Education, 2nd editio edition, 1994.
- ²⁶ IBM. IBM ILOG CPLEX Optimization Studio CPLEX User Manual. Technical report, 2015.
- ²⁷ John Warnock, David McMillan, James A. Pilgrim, and Sally Shenton. Review of offshore cable reliability metrics. In *Proceedings of the 13th IET International Conference on AC and DC Power Transmission (ACDC)*, pages 1–6, 2017.
- ²⁸ Statista. Monthly average electricity prices in Great Britain (GB) from 2015 to 2019, 2019.
- ²⁹ ABB. XLPE Submarine Cable Systems Attachment to XLPE Land Cable Systems - User’s Guide, 2018.
- ³⁰ Vatenfall. Ormonde Offshore Wind Farm.
- ³¹ Vatenfall. Horns Rev 1 Offshore Wind Farm.
- ³² Ørsted. West of Duddon Sands Offshore Wind Farm.

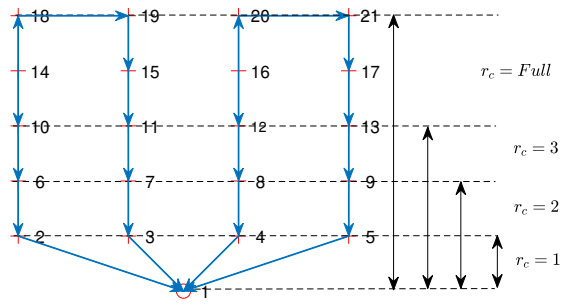


Figure 1. Reliability level definition.

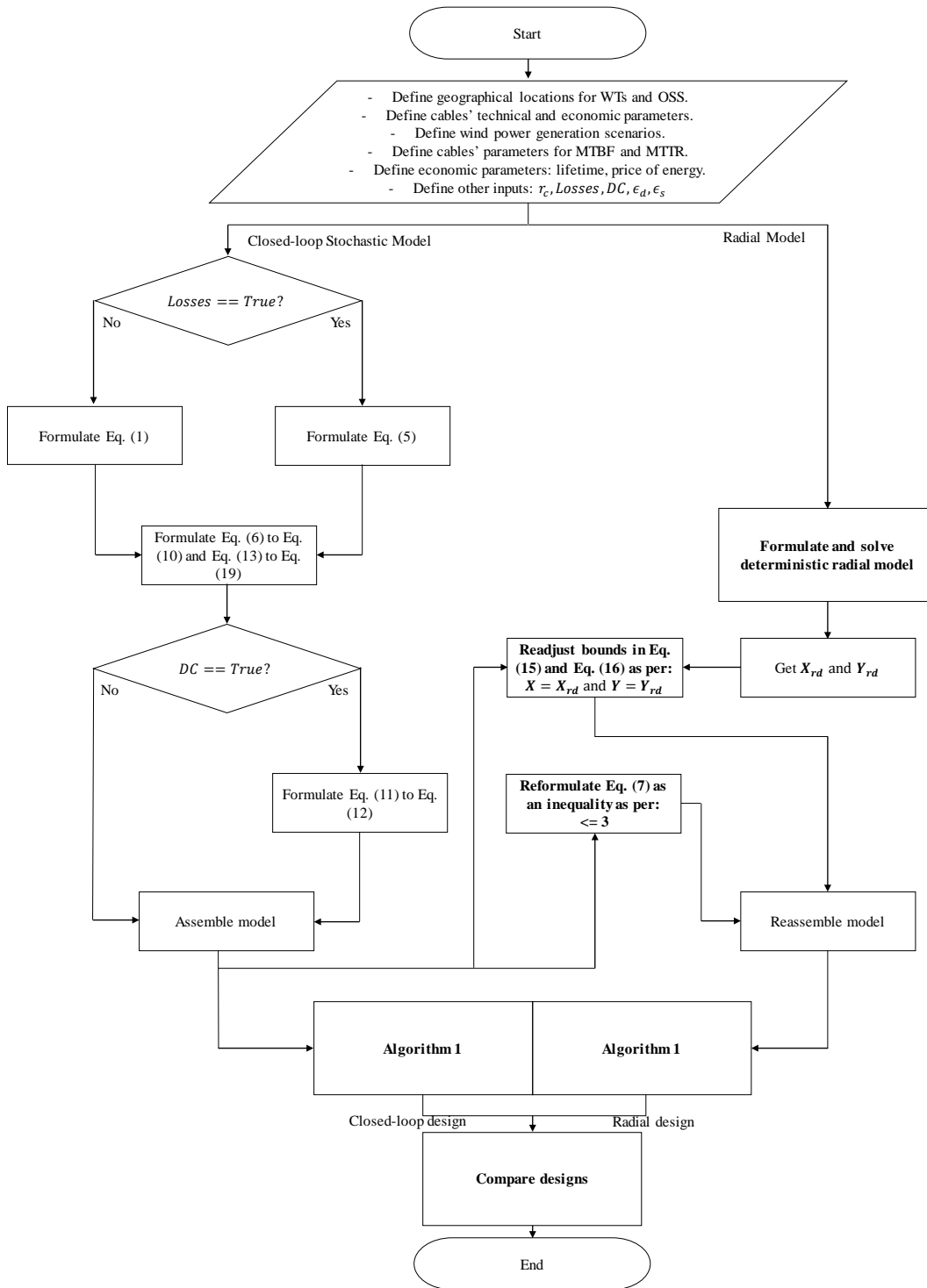
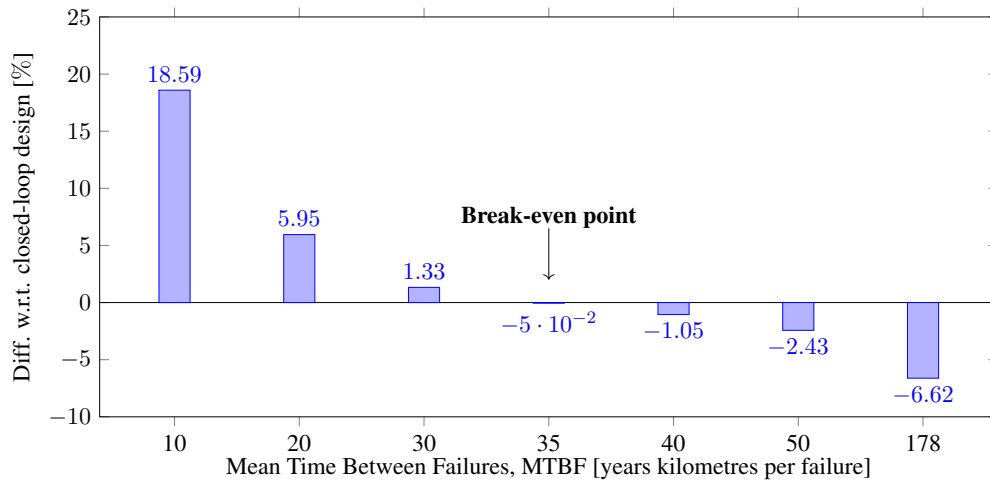
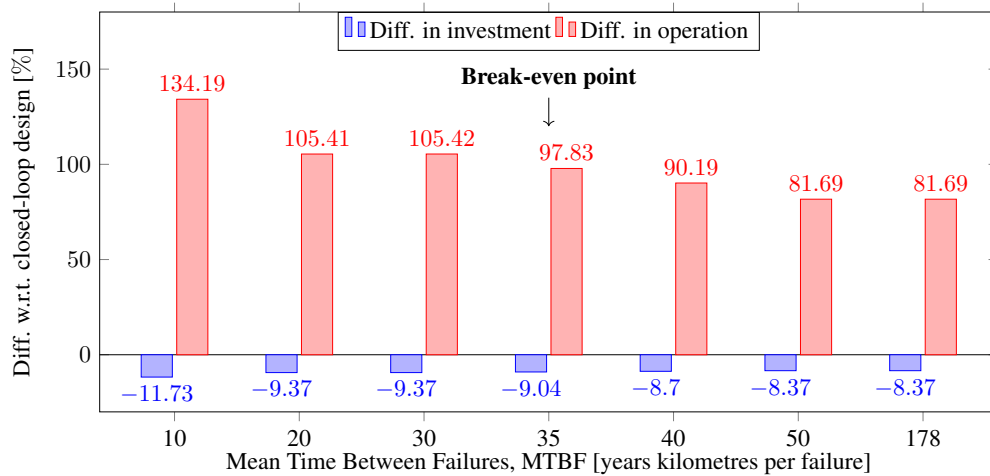


Figure 2. Optimization framework for comparing collection system topology.

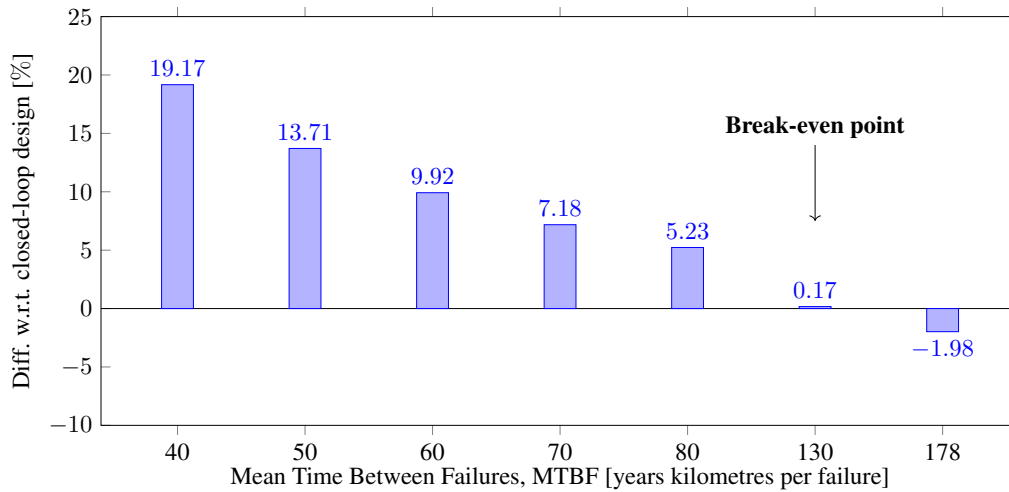


(a) Comparison of objective function (1) between closed-loop and radial designs. (Positive percentages mean savings from closed-loop design)

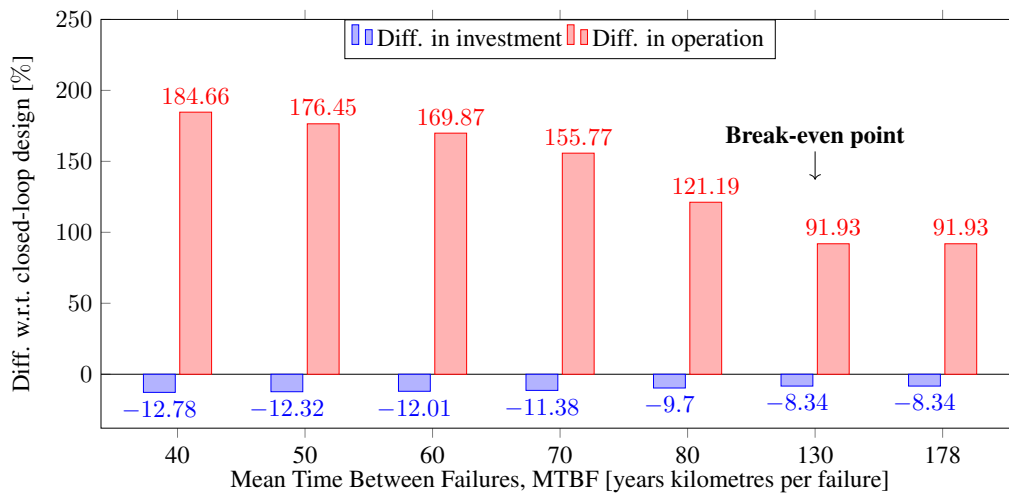


(b) Comparison of investment and operations costs between closed-loop and radial designs. (Positive percentages mean savings from closed-loop design)

Figure 3. Sensitivity analysis with reliability level $r_c = 1$ for Ormonde OWF.



(a) Comparison of objective function (1) between closed-loop and radial designs. (Positive percentages mean savings from closed-loop design)



(b) Comparison of investment and operations costs between closed-loop and radial designs. (Positive percentages mean savings from closed-loop design)

Figure 4. Sensitivity analysis with full reliability for Ormonde OWF.

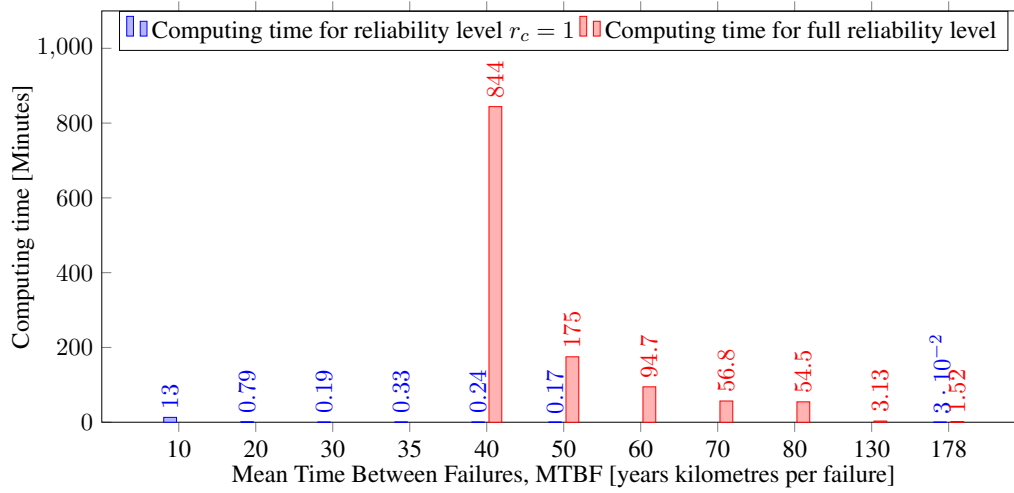
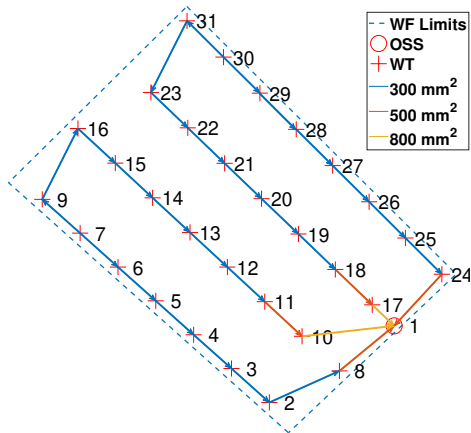
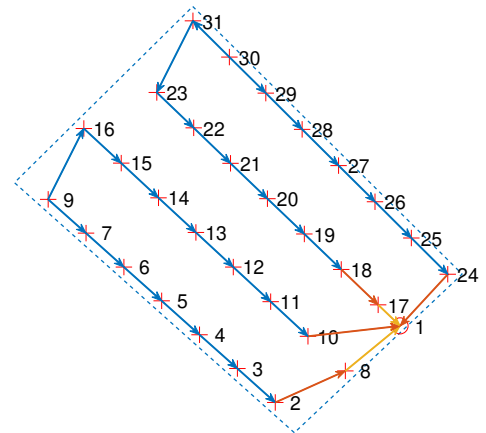


Figure 5. Computing times for Ormonde OWF stochastic closed-loop design.

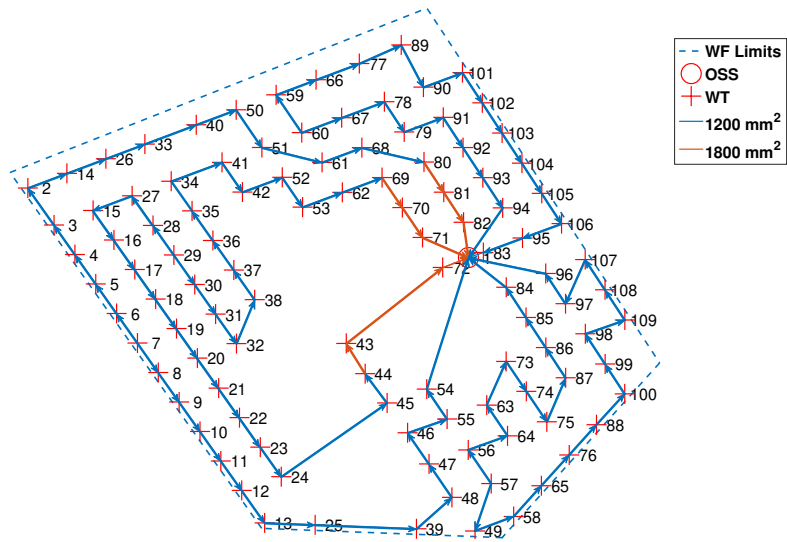


(a) Investment and Operation

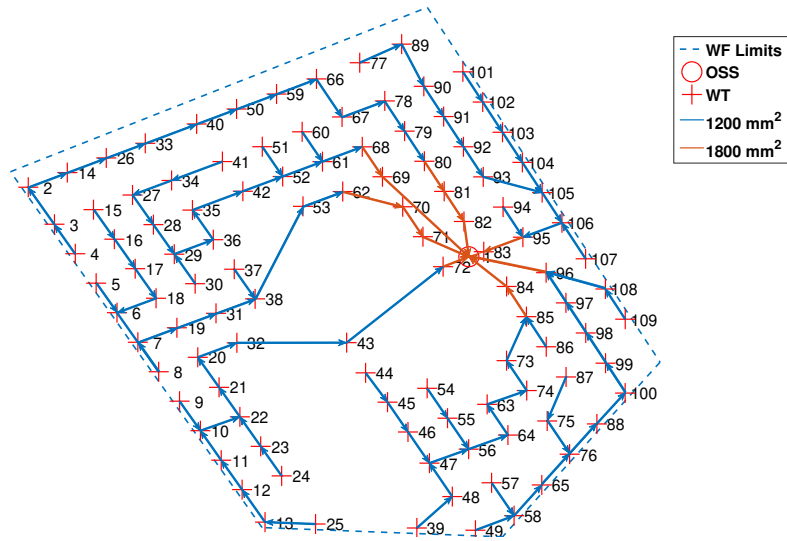


(b) Investment, Electrical losses, and Operation

Figure 6. Sensitivity analysis for objective function in Ormonde OWF. MTBF=178.



(a) Closed-loop design for West of Duddon Sands with MTBF=178



(b) Radial design for West of Duddon Sands

Figure 7. Collection system designs for West of Duddon Sands with objective function (1).

Table 1. Wind power generation scenarios.

Scenario	Magnitude [p.u.]	Duration [h]
1	1	65,700
2	0.5	91,980
3	0.2	91,980
4	0	13,140

Table 2. Data inputs for Ormonde OWF.

P_n	V_n	U	C	n_w	ν	σ	ϕ	ϵ_d	ϵ_s
5 MW	33 kV	{530, 655, 775} A	{450, 510, 570} kEuro km ⁻¹	30	6	10	4	0.2%	0.2%

Table 3. Power flow models comparison for Ormonde OWF.

MTBF	Total expenses Eq. (1)		Investment		Operation	
	Difference [Euro]	Difference [%]	Difference [Euro]	Difference [%]	Difference [Euro]	Difference [%]
10	0	0	0	0	0	0
20	8,000	0.08	32,200	0.37	-24,200	-1.79
30	16,090	0.17	32,200	0.37	-16,110	-1.79
40	23,920	0.25	64,200	0.74	-40,280	-5.52
50	31,970	0.34	64,200	0.74	-32,230	-5.27
178	55,140	0.62	64,200	0.74	-9,060	-5.27

Table 4. Data inputs for Horns Rev 1 OWF

P_n	V_n	U	C	n_w	v	σ	ϕ	ϵ_d	ϵ_s
2 MW	33 kV	{420, 530} A	{410, 450} kEuro km ⁻¹	80	6	10	10	0.2%	0.2%/4%

Table 5. Results with reliability level $r_c = 1$ for Horns Rev 1 OWF.

MTBF	Diff. in total expenses Eq. (1) [%]	Diff. in investment [%]	Diff. in operation [%]	Computing time closed-loop [min]
90	-0.80	-3.34	91.14	359
178	-2.01	-3.31	90.90	43

Table 6. Results with full reliability level for Horns Rev 1 OWF.

MTBF	Diff. in total expenses Eq. (1) [%]	Diff. in investment [%]	Diff. in operation [%]	Computing time closed-loop [h]
178	1.13	-3.43	83.01	2.47

Table 7. Data inputs for West of Duddon Sands OWF

P_n	V_n	U	C	n_w	ν	σ	ϕ	ϵ_d	ϵ_s
3.6 MW	33 kV	{875, 1050} A	{630, 770} kEuro km ⁻¹	108	10	25	10	5%	6%

Table 8. Results with reliability level $r_c = 1$ for West of Duddon Sands OWF.

MTBF	Diff. in total expenses Eq. (1) [%]	Diff. in investment [%]	Diff. in operation [%]	Computing time closed-loop [h]
178	-0.67	-1.65	96.46	0.90